

# High pressure effects on isotropic Nd<sub>2</sub>Fe<sub>14</sub>B magnet

Masaki Mito<sup>1,\*</sup> and Takayuki Tajiri<sup>2</sup>

<sup>1</sup>Graduate School of Engineering, Kyushu Institute of Technology, Kitakyushu 804-8550, Japan

<sup>2</sup>Faculty of Science, Fukuoka University, Fukuoka 814-0180, Japan

We conducted the structural analyses of an isotropic Nd<sub>2</sub>Fe<sub>14</sub>B magnet (the exact chemical formula is Nd<sub>2.0</sub>Fe<sub>14.1</sub>B) consisting of nanocrystals, with the size of approximately 30 nm, under pressures ( $P$ 's) up to 4.3 GPa. In the magnetization measurements up to 9.3 GPa, it has already been known that the coercive field  $H_c$  at 300 K increases almost linearly against the pressure, and the increase in  $H_c$  saturates at around  $P = 3$  GPa. The present experiments show that the crystalline strain increases for  $P < 1$  GPa. Afterward, the crystalline size ( $D$ ) starts to decrease with increasing pressure, and the reduction tends to saturate at above approximately 3 GPa, suggesting that the change in  $M_s$  is actually related with both the change in strain and that in  $D$ . Consequently, the change in  $H_c$  is understood by the decrease in the saturation magnetization  $M_s$  within the framework of the constant anisotropy of the single domain phase.

## 1 Introduction

The Nd<sub>2</sub>Fe<sub>14</sub>B magnet is currently one of the most attractive permanent magnets with high coercive field ( $H_c$ ) [1-3]. The ferromagnetic transition temperature ( $T_C$ ) of Nd<sub>2</sub>Fe<sub>14</sub>B is generally recognized as 586 K [1-3]. The main phase has the space group  $P4_2/mnm$ , and there are four Nd<sub>2</sub>Fe<sub>14</sub>B units per one unit cell [3, 4]. To utilize a Nd<sub>2</sub>Fe<sub>14</sub>B magnet at high temperatures (e.g., for a car engine), it is necessary to disrupt the decrease in  $H_c$  at around 500 K. Our interest is to increase  $H_c$  by the use of external stress.

The effect of shock wave compression on the strain in the Nd<sub>2</sub>Fe<sub>14</sub>B magnet was investigated recently [5], and the effect of loading at low temperature for rapidly quenched Nd<sub>2</sub>Fe<sub>14</sub>B nanocrystalline magnets has also been studied [6]. Thus, from the viewpoint of basic physics, the effect of strain on Nd<sub>2</sub>Fe<sub>14</sub>B magnets has been attractive. In 1987, the change in  $T_C$  against the pressure ( $P$ ) for a polycrystalline sample,  $dT_C/dP = -26.5$  K/GPa, was investigated by Kamarad *et al* [7]. In amorphous Nd<sub>2</sub>Fe<sub>14</sub>B [ $T_C(P=0) = 422$  K],  $dT_C/dP = -48$  K/GPa [8]. However, there has never been the study for the pressure effect on  $H_c$ . Now, isotropic bond magnets are suitable for attempting to change  $H_c$  by manipulating the structure of the main phase. Given these background, we investigate the change in  $H_c$  under hydrostatic pressure for an isotropic Nd<sub>2</sub>Fe<sub>14</sub>B magnet and examine the magnetostructural correlation as a function of pressure [9].

## 2 Experiment

A target Nd<sub>2</sub>Fe<sub>14</sub>B bond magnet is called MQP-B 20052-070 (Nd<sub>2.0</sub>Fe<sub>14.1</sub>B; MQP, Magnequench, A Division of Neo Material Technologies Inc.); this magnet is used as the spindle motor in hard disks, power tools, and so on. The density is  $7.61 \pm 0.20$  g/cm<sup>3</sup>. The median size of the nanoparticles aggregated at the sample surface, observed from the SEM image, is approximately 60 nm. The crystalline size  $D$  in the whole sample is evaluated to be approximately 30 nm in the structural experiment.

Powder X-ray diffraction (XRD) analysis under pressures was conducted at room temperature using a

synchrotron radiation XRD system with a cylindrical imaging plate at the Photon Factory (PF) at the Institute of Materials Structure Science, High Energy Accelerator Research Organization (KEK) [10]. The wavelength of the incident X-ray was 0.88571 Å. Pressure was applied using a CuBe diamond anvil cell, containing the Nd<sub>2</sub>Fe<sub>14</sub>B nanocrystals along with a ruby as a manometer and fluorinated oil as the pressure-transmitting medium.

## 3 Results and Discussion

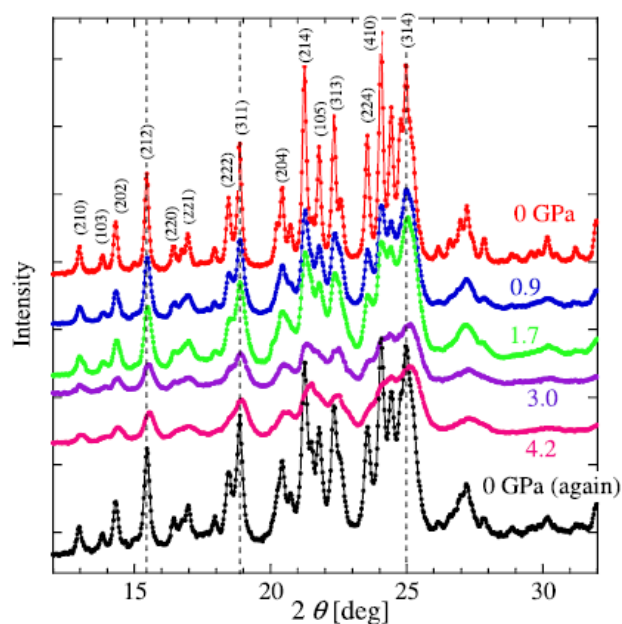


Fig. 1: Diffraction pattern of Nd<sub>2.0</sub>Fe<sub>14.1</sub>B bond magnet for  $P \leq 4.2$  GPa. The pattern at  $P = 0$  GPa is explained by a crystal structure of  $P4_2/mnm$  with  $a = 8.795$  Å and  $c = 12.188$  Å. The plane indices are presented for the diffraction peaks below  $2\theta = 25^\circ$ . Three broken lines are guides to the eye to confirm the pattern shift.

Figure 1 shows the XRD pattern at room temperature for Nd<sub>2.0</sub>Fe<sub>14.1</sub>B. We estimated the crystallite size  $D$  and strain according to the Williamson-Hall plot, and their results are shown in Fig. 2. At  $P = 0$  GPa, the crystallite

size  $D$  was estimated to be  $27.5 \pm 2.8$  nm. For  $P < 1$  GPa, the strain is enhanced, whereas for  $P > 1$  GPa, the magnitude tends to be saturated. After the saturation of the strain magnitude,  $D$  begins to decrease and, for  $P > 3$  GPa, its reduction also tends to be saturated. Indeed, both the saturation of the increase in  $H_c$  and the saturation in the change in  $D$  occur at the same pressure of approximately 3 GPa. We consider that by applying pressure, some atomic sites deviate from the positions with translation symmetry, resulting in the reduction in crystallinity as seen in Fig. 1. This influence appears in the lattice parameters and in  $D$ .

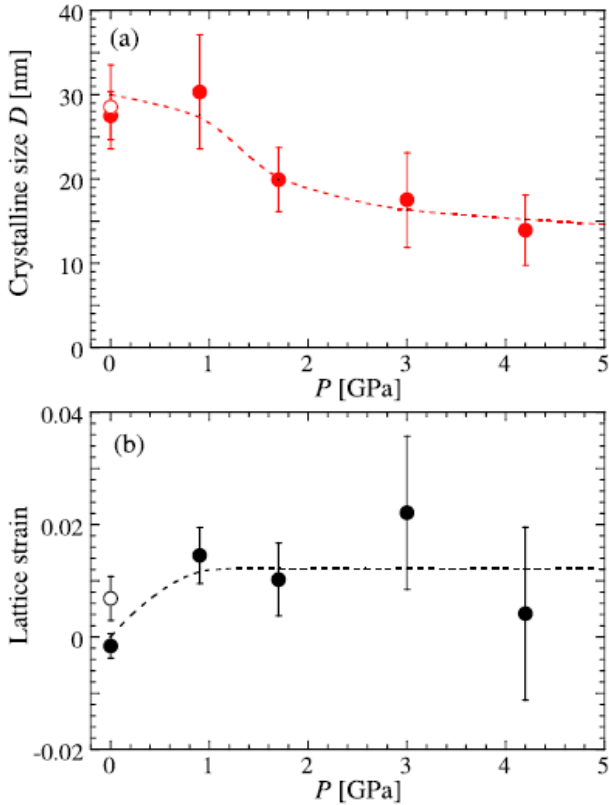


Fig. 2: Pressure dependence of crystalline size  $D$  (a) and strain (b) of  $\text{Nd}_{2.0}\text{Fe}_{14.1}\text{B}$  bond magnet for  $P \leq 4.2$  GPa. The broken curves are guides for the eyes. In both (a) and (b), open symbols stand for the data after releasing 4.2 GPa.

Figure 3 also shows the pressure dependence of the lattice parameters obtained via the peak angles of the distinguishable diffraction peaks. For  $P \leq 1.7$  GPa, contraction within the  $ab$  plane is dominant, whereas for  $P > 1.7$  GPa, the volume contraction originates in contraction along the  $c$ -axis rather than that within the  $ab$  plane (see Fig. 4).

The increase in  $H_c$  for  $\text{Nd}_{2.0}\text{Fe}_{14.1}\text{B}$  at room temperature appears for  $P < 4$  GPa, with a constant value of  $\mu_0 M_s H_c$ .  $H_c$  is enhanced within the framework of the Stoner-Wohlfarth model with a constant  $K_u$  [11]. Its change in  $H_c$  occurs in the pressure region, where anisotropic shrinkage occurs, and it cannot be scaled with one lattice parameter among  $a$ ,  $c$ , and  $V$ . After the change

in lattice strain disappears,  $D$  starts to decrease largely. We stress that the change in  $H_c$  is the most similar to that in  $D$  among a series of structural parameters. Indeed, the change in  $D$  is surely related with the change in  $c$ . In order to elucidate the magneto-structural correlation, we have to pursue each atomic position at pressures. We are planning the structural analysis at pressure of below 1 GPa, where the lattice strain exhibits a prominent change.

According to the literature, amorphization results in reduction of both  $H_c$  and  $T_C$  [12]. We remark that the reduction in crystallinity mainly brings about reduction of both  $H_c$  and  $T_C$  in the present study. Indeed, the structural change accompanying the reduction in crystallinity under hydrostatic pressure reduces  $T_C$  [9], and it degrades the performance at around 500 K. However, if we consider the magnetic properties below 400 K, the temporal increase in  $H_c$  is realized.

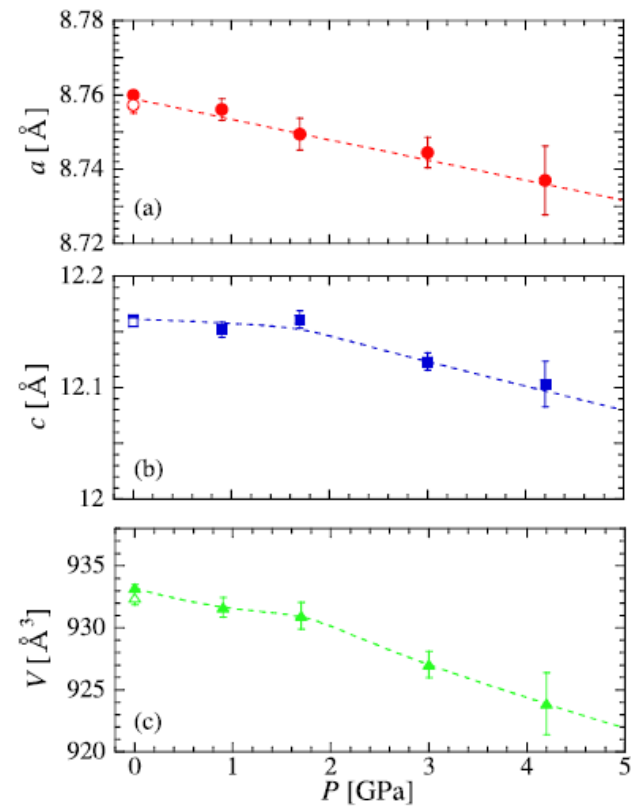


Fig. 3: Pressure dependence of the lattice parameters ( $a$ ,  $c$ ,  $V$ ) of  $\text{Nd}_{2.0}\text{Fe}_{14.1}\text{B}$  bond magnet for  $P \leq 4.2$  GPa. In (a)-(c), open symbols stand for the data after releasing 4.2 GPa. The broken lines are guides for the eyes.

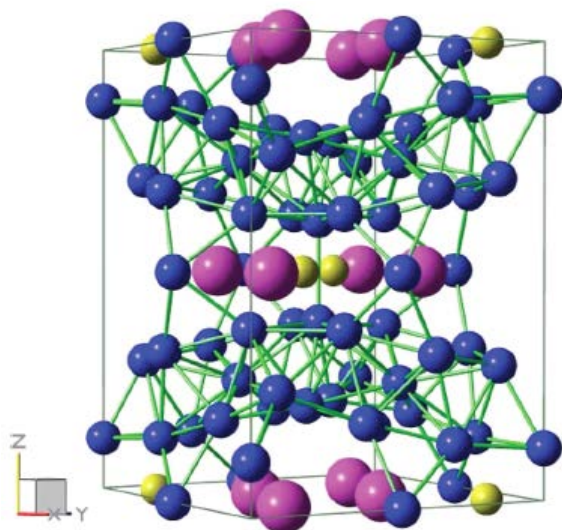


Fig. 4: Crystal structure displayed referring to the literature. Purple, blue, and yellow spheres represent Nd, Fe, and B atoms, respectively.

London, Ser. A **240**, 599 (1948).

[12] A. Teplykh, Y. Chukalkin, S. Lee, S. Bogdanov, N. Kudrevatykh, E. Rosenfeld, Y. Skryabin, Y. Choi, A. Andreev, and A. Pirogov, *J. Alloys Compd.* **581**, 423 (2013).

\*mitoh@mns.kyutech.ac.jp

#### Acknowledgement (option)

This work was supported by MEXT KAKENHI [Grant-in-Aid for Scientific Research (B) (No. 26289091) and Grant-in-Aid for Scientific Research on Innovative Areas “Bulk Nanostructured Metals” (No. 25102709)]. M.M. acknowledges NSK Ltd. for supplying the Ti alloy and Magnequench International for supplying the  $\text{Nd}_{2.0}\text{Fe}_{14.1}\text{B}$  bond magnet.

#### References

- [1] M. Sagawa, S. Fujimura, N. Togawa, H. Yamamoto, and Y. Matsuura, *J. Appl. Phys.* **55**, 2083 (1984).
- [2] J. J. Croat, J. F. Herbst, R. W. Lee, and F. E. Pinkerton, *J. Appl. Phys.* **55**, 2078 (1984).
- [3] J. F. Herbst, *Rev. Mod. Phys.* **63**, 819 (1991).
- [4] J. F. Herbst, J. J. Croat, F. E. Pinkerton, and W. B. Yelon, *Phys. Rev.* **29**, 4176 (1984).
- [5] L. Yan-Feng, Z. Ming-Gang, L. Wei, Z. Dong, L. Feng, C. Lang, W. Jun-Ying, Q. Yan, and D. An, *Chin. Phys. Lett.* **30**, 097501 (2013).
- [6] C. Bing Rong, Y. Q. Wu, D. Wang, Y. Zhang, N. Poudyal, M. J. Kramer, and J. P. Liu, *J. Appl. Phys.* **111**, 07A717 (2012).
- [7] J. Kamarad, Z. Arnold, and J. Schneider, *J. Magn. Magn. Mater.* **67**, 29 (1987).
- [8] K. Fukamachi, K. Shirakawa, Y. Satoh, T. Masumoto, and T. Kaneko, *J. Magn. Magn. Mater.* **54–57**, 231–232 (1986).
- [9] M. Mito, H. Goto, K. Nagai, K. Tsuruta, H. Deguchi, T. Tajiri, and K. Konishi, *J. Appl. Phys.* **118**, 145901 (2015).
- [10] A. Fujiwara, K. Ishii, T. Watanuki, H. Suematsu, H. Nakao, K. Ohwada, Y. Fujii, Y. Murakami, T. Mori, H. Kawada et al., *J. Appl. Crystallogr.* **33**, 1241 (2000).
- [11] E. Stoner and E. Wohlfarth, *Philos. Trans. R. Soc.*